Communication

Many-Body Polarization Effects and the Membrane Dipole Potential

Edward Harder, Alexander D. MacKerell Jr., and Benoît Roux

J. Am. Chem. Soc., **2009**, 131 (8), 2760-2761• DOI: 10.1021/ja806825g • Publication Date (Web): 06 February 2009

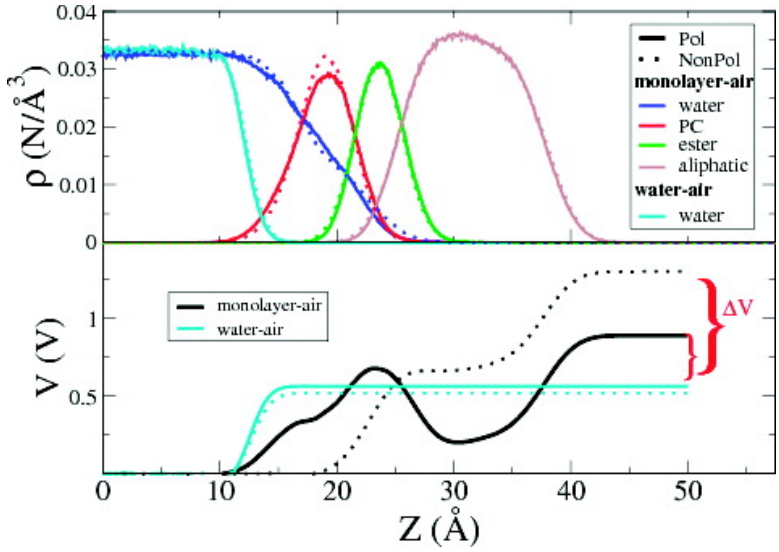

More About This Article

Additional resources and features associated with this article are available within the HTML version:

- Supporting Information
- Access to high resolution figures
- Links to articles and content related to this article
- Copyright permission to reproduce figures and/or text from this article

View the Full Text HTML

J|A|C|S COMMUNICATIONS

Published on Web 02/06/2009

Many-Body Polarization Effects and the Membrane Dipole Potential

Edward Harder,[†] Alexander D. MacKerell, Jr.,*[,‡] and Benoît Roux*[,†]

Department of Biochemistry and Molecular Biology, Center for Integrative Science, University of Chicago, Chicago, Illinois 60637, and Department of Pharmaceutical Sciences, School of Pharmacy, University of Maryland, Baltimore, Maryland 21201

Received August 28, 2008; E-mail: alex@outerbanks.umaryland.edu; roux@uchicago.edu

A large positive potential in the interior of membranes[1,2] is responsible for the difference in permeability between negative and positive hydrophobic ions.[3] This potential, referred to as the membrane dipole potential, is also thought to play a role in controlling the association of proteins at the membrane surface and the structure and function of membrane bound proteins.[4]

Molecular simulations of atomic resolution models can provide valuable insight into structural details not easily accessible from experiment. The simulated atomic structures and the assigned atomic charges can be used to determine the average electrostatic potential profile along the interface normal. Unfortunately, the dipole potential computed from all-atom trajectories based on current force fields is considered too positive with respect to experiment.[5] These force fields try to approximate many-body electronic polarization effects in an average way using atomic partial charges that are invariant to their electrostatic environment. By accounting for these effects in the framework of a fully polarizable lipid−water simulation, it is hoped that the gap between simulation and experiment can be bridged, allowing for an improved understanding of the physical nature of lipid membranes.

Although the absolute electrostatic potential difference between two media is not by itself a meaningful measurable quantity,[6] the shift in the interfacial potential before ($V_{water-air}$) and after ($V_{mono-air}$) spreading a lipid monolayer on a water−air interface,

$$\Delta V = V_{mono-air} - V_{water-air}, \quad (1)$$

is unambiguous and provides pertinent information about membranes. The experimental measure of this monolayer dipole potential, which ranges between 0.3 and 0.4 V in phosphatidylcholine lipids,[7] forms the comparative basis of this study.

Molecular dynamics simulations of a DPPC monolayer−air and water−air system were performed with the program CHARMM.[8] One set of simulations was performed with a potential function accounting explicitly for induced electrostatic polarizability, by using a model based on classical Drude oscillators (Pol).[9,10] A second set of simulations was performed with the nonpolarizable CHARMM lipid force field[11] and the TIP3P water model[12] (NonPol). Details of the system preparation are provided in the Supporting Information (SI).

Data are averaged over the pair of interface regions and is plotted along the interface normal in Figure 1. The heavy atom particle density profile is shown in panel A. The total system density is partitioned into four chemical groups: water, the phosphatidylcholine headgroup (PC), the esterified glycerol backbone (ester), and the aliphatic lipid tails. At this level of structural resolution the density profiles for both the Pol and NonPol models are similar. The electrostatic potential profile is calculated from the average

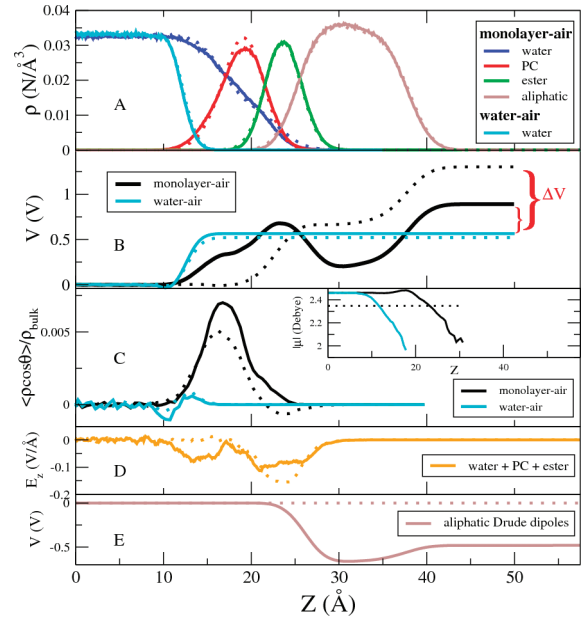

Figure 1. Data computed from simulations of a monolayer-air and water−air system. Solid and dotted lines correspond to the Pol and NonPol models, respectively. The heavy atom particle density is in panel A, the dipole potential is in panel B, the water orientational order and dipole magnitude (inset) are in panel C, panel D is the average electric field from polar molecular groups, and panel E is the potential from electrostatic polarization of the hydrocarbon tails. Monolayer area/lipid is 63 Å^2.

system charge density as a solution to the Poisson equation[9] and plotted in panel B. Quantitatively, the monolayer-air potential difference is 1.3 V for the NonPol model and 0.9 V for the Pol model. According to eq 1, subtracting the water−air reference state ($V_{water-air}$) from $V_{mono-air}$ gives the experimental observable, ΔV, which is 0.8 V for the NonPol model. In contrast, ΔV is 0.35 V for the Pol model, in excellent agreement with the experimental range 0.3−0.4 V[5] (further details regarding this calculation are given in the SI). Partitioning the charge density according to the particle density in panel A gives the individual, additive, molecular contributions for each group (Table 1 in the SI). The polarization of the zwitterionic PC headgroup gives the largest contribution to the lipid potential (−2.9 V for Pol and −2.4 V for NonPol). This large potential is due to the tilt of the headgroup away from the interface plane toward the water phase. The P−N vector is tilted by 26 in the Pol model and 16 in the NonPol model. The projection of the PC headgroup in the Pol model is consistent with recent experimental findings.[13]

The large contribution from the PC group is offset by the dielectric response of the surrounding water environment. For both water models, the bare water−air interface potential ($V_{water-air}$) is ∼0.5 V.[9] Though difficult to measure unambiguously[6] and model

[†] University of Chicago.
[‡] University of Maryland.

10.1021/ja806825g CCC: $40.75

sensitive,[14] this is the proper offset value that must be used in eq 1 to determine the experimentally accessible observable, ΔV, associated with the monolayer. The monolayer polarizes water molecules at the interface leading to a 4.2 and 2.6 V contribution to the potential, from the charge density of the Pol and NonPol water models, respectively. Orientational polarization of water is measured by a density weighted order parameter (panel C)[15] where θ is the angle between the dipole of water and the interface normal. The inset shows the average magnitude of the water molecular dipole. At the interface, the dipole relaxes from 2.4 D to the gas phase value (1.85 D), an effect not accessible to the NonPol water model. There is also significant concerted orientational ordering of water at the interface, which is enhanced in the Pol model.

Isolating the effects of induced polarization in the ester region is not entirely straightforward. The charges of the NonPol ester model are empirically adjusted to yield a number of macroscopic properties at the expense of its isolated molecular dipole.[16] For comparison, a nonpolarizable charge model is built (ESTERμ) that accurately reflects the gas phase charge distribution of the ester group (see SI). The accuracy of the charge model is tested on 27 isolated rotamers of a compound representative of the lipid ester region. The component of the molecular dipole that approximately aligns with the interface normal of the monolayer simulation is plotted in Figure 2. Both the Pol and ESTERμ models reproduce well the QM model dipole. The ESTERμ charges were subsequently applied to structures obtained from the Pol model simulation. The contribution to the dipole potential from the ESTERμ charges is 0.25 V (compared to 0.7 V for the NonPol model), whereas the Pol model contribution is marginally negative (−0.1 V). Since the models share identical atomic structures and nearly identical gas phase dipoles, this difference in potential can be attributed mainly to electrostatic polarization by the monolayer environment, reorienting the dipole of the Pol model to lie nearly parallel, on average, with the plane of the interface.

The orientational and induced polarization from the headgroups and water molecules give rise to a net residual electric field in the interior of the monolayer (panel D). This electric field, for both the Pol and NonPol models, is directed toward the water phase and overlaps with the hydrocarbon chains. In the Pol model, the contribution to the dipole potential from the hydrocarbon chains in response to this electric field is ∼0.5 V (Panel E). This value, which is similar in magnitude to the total monolayer potential, is missing entirely from the NonPol model. Because the hydrocarbon chains do not carry a significant permanent dipole, any electrostatic response from this region is primarily due to induced polarization effects.[17] This response is reflected in the bulk hydrocarbon dielectric constant which is seriously in error in the NonPol model ($\varepsilon \approx 1$) and accurately represented in the Pol model ($\varepsilon \approx 2$).[17]

In summary, the present study indicates that the inclusion of induced polarization effects is essential to develop accurate models of membranes. With the present model a lipid interface dipole potential that is in quantitative agreement with experiment was achieved. Electrostatic polarization in the interior of the lipid is found to significantly buffer the positive dipole potential. It is important to emphasize that parameters of the Pol model were not adjusted in any way to empirically fit the experimental value. Therefore, the quantitative agreement appears to be a consequence of an improved treatment of the microscopic physics of the system to account for induced polarization. We anticipate that polarizable models will allow for a more reliable picture of molecular interactions and additional insights into properties of lipids and their relationship to atomic level features of the system.

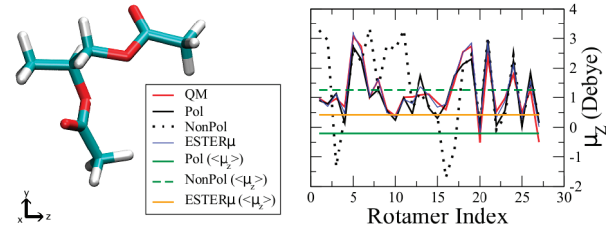

Figure 2. Dipole for the 27 rotamers of the molecular model of the lipid ester region. The QM dipole is computed at the B3LYP/aug-cc-pVDZ level. Averages (⟨ ⟩) from the simulation are also shown.

Acknowledgment. This work was supported by Grant GM 072558 from the National Institute of Health. Computations conducted at NCSA.

Supporting Information Available: Computational details, dipole potential constituents, and methyl acetate dipole. This material is available free of charge via the Internet at http://pubs.acs.org.

References

(1) (a) Liberman, Y. A.; Topaly, V. P. *Biofizika* **1969**, *14*, 452–461. (b) Haydon, D. A.; Myers, V. B. *Biochim. Biophys. Acta* **1973**, *307*, 429–443.
(2) (a) Wang, L.; Bose, P. S.; Sigworth, F. J. *Proc. Natl. Acad. Sci. U.S.A.* **2006**, *103*, 18528–18533. (b) Gawrisch, K.; Ruston, D.; Zimmerberg, J.; Parsegian, V. A.; Rand, R. P.; Fuller, N. *Biophys. J.* **1992**, *61*, 1213–1223. (c) Schamberger, J.; Clarke, R. J. *Biophys. J.* **2002**, *82*, 3081–3088.
(3) Pickar, A. D.; Benz, R. *J. Membr. Biol.* **1978**, *44*, 353–376.
(4) Brockman, H. *Chem. Phys. Lipids* **1994**, *73*, 57–79.
(5) Siu, S. W. I.; Vacha, R.; Jungwirth, P.; Rockman, R. A. *J. Chem. Phys.* **2008**, *128*, 125103.
(6) (a) Gibbs, J. W. *The Scientific Papers of J. Willard Gibbs*; Dover, NY, 1961; Vol. 1, p 429. (b) Guggenheim, E. A. *J. Phys. Chem.* **1929**, *33*, 842–849. (c) Pethica, B. A. *Phys. Chem. Chem. Phys.* **2007**, *9*, 6253–6262. (d) Harder, E.; Roux, B. *J. Chem. Phys.* **2008**, *129*, 234706.
(7) Smaby, J. M.; Brockman, H. L. *Biophys. J.* **1990**, *58*, 195–204.
(8) MacKerell, A. D., Jr.; Brooks, B.; Brooks, C. L., III; Nilsson, L.; Roux, B.; Won, Y.; Karplus, M. *CHARMM: The Energy Function and Its Parameterization with an Overview of the Program. In "Encyclopedia of Computational Chemistry, Vol.1"*; John Wiley & Sons: Chichester, 1998.
(9) Lamoureux, G.; Harder, E.; Vorobyov, I. V.; Roux, B.; MacKerell, A. D., Jr *Chem. Phys. Lett.* **2006**, *418*, 245–249.
(10) Drude, P. *The Theory of Optics*; Longmans, Green: New York, 1902.
(11) Schlenkrich, M.; Brickman, J.; MacKerell, A. D., Jr.; Karplus, M. An Empirical Potential Energy Function for Phospholipids: Criteria for Parameter Optimization and Applications. In *Biological Membranes: A Molecular Perspective from Computation and Experiments*; Merz, K.; Roux, B., Eds.; Birkhauser: Cambridge, MA, 1996.
(12) Jorgensen, W. L.; Chandrasekhar, J.; Madura, J. D.; Impey, R. W.; Klein, M. L. *J. Chem. Phys.* **1983**, *79*, 926–935.
(13) Semchyschyn, D. J.; Macdonald, P. M. *Magn. Reson. Chem.* **2004**, *42*, 89–104.
(14) Kathmann, S. M.; Kuo, I-F. W.; Mundy, C. *J. Am. Chem. Soc.* **2008**, *130*, 16556–16561.
(15) Feller, S. E.; Pastor, R. W.; Rojnuckarin, A.; Bogusz, S.; Brooks, B. R. *J. Phys. Chem.* **1996**, *100*, 17011–17020.
(16) MacKerell, A. D., Jr *J. Comput. Chem.* **2004**, *25*, 1584–1604.
(17) Vorobyov, I. V.; Anisimov, V. M.; MacKerell, A. D., Jr. *J. Phys. Chem. B* **2005**, *109*, 18988–18999.

JA806825G